Article

J. Biol. Regul. Homeost. Agents. 2024; 38(5): 3777–3790
https://doi.org/10.23812/j.biol.regul.homeost.agents.20243805.298

Coixol Ameliorates Rheumatoid Arthritis by Regulating Macrophage Polarization by Suppressing the TLR4/NF-κB Pathway

Baoxin Wang[1], Jingling Cai[2], Xiaojiang Guo[1], Xiaolei Shen[1], Chunxiang Niu[1], Lu Peng[3], Fei Qu[1,*]

[1]Department of Emergency, Jiaxing Hospital of Traditional Chinese Medicine, 314015 Jiaxing, Zhejiang, China
[2]Department of Geriatrics, Hubei Provincial Hospital of Traditional Chinese Medicine, 430060 Wuhan, Hubei, China
[3]Department of Traditional Chinese Medicine and Rheumatology, People's Hospital of Ningxiang City, 410699 Ningxiang, Hunan, China
*Correspondence: 383207932@qq.com (Fei Qu)
Published: 1 May 2024

Background: Coixol (COI) is derived from *C. lacryma-jobi var. ma-yuen* (Rom.Caill.) Stapf and has been shown with protective effects on rheumatoid arthritis (RA). However, the detailed mechanisms of COI on RA remain unknown. The current study aimed to assess the therapeutic effect and possible mechanism of COI on RA.

Methods: A collagen-induced arthritis (CIA) rat model was established, and COI was administered to CIA rats orally. The therapeutic effects of COI on RA were assessed based on arthritis score and paw volume, pathological staining and the levels of inflammatory factors. Then, the effects of COI on M1 macrophages (Mφ) polarization were evaluated through measuring the levels of M1Mφ-related factors, detecting the proportion of M1Mφ in spleen and synovium. Furthermore, the inhibitory effect of COI on M1Mφ polarization was verified *in vitro* and the changes in toll-like receptor 4 (TLR4)/nuclear factor-kappaB (NF-κB) pathway in M1Mφ after COI treatment was evaluated through detecting the related levels of proteins and genes. Additionally, the inhibitory effect of COI on NF-κB p65 activation in M1Mφ was assessed through detecting the nucleus transition of NF-κB p65 and the NF-κB transcriptional activity.

Results: COI decreased arthritis score and paw volume, improved the pathological changes, and reduced the levels of inflammatory factors in CIA rats ($p < 0.01$). Besides, COI treatment reduced the proportion of M1Mφ in the spleen and synovium ($p < 0.01$). *In vitro* studies suggested that COI decreased the proportion of M1Mφ and reduced the production of pro-inflammatory cytokines ($p < 0.05$, $p < 0.01$, respectively). Besides, COI treatment lowered the protein levels of TLR4/NF-κB pathway-related factors and downregulated the gene expression of downstream cytokines ($p < 0.05$, $p < 0.01$, respectively). Furthermore, COI treatment inhibited the nucleus transition of NF-κB p65 and diminished the transcriptional activity of NF-κB ($p < 0.05$).

Conclusions: COI exhibits a significant therapeutic effect on RA. The anti-inflammatory mechanism of COI on RA is associated with inhibiting TLR4/NF-κB-mediated M1Mφ polarization.

Keywords: COI; RA; M1Mφ polarization; TLR4/NF-κB pathway

Introduction

Rheumatoid arthritis (RA) is primarily accompanied by synovial hyperplasia and persistent synovitis. These can invade and damage cartilage and bone, causing joint dysfunction and even loss of function [1]. Our understanding of the complex pathogenesis of RA is continually evolving [2]. Although the drugs used in current treatment strategies can alleviate RA symptoms and slow down its progression, they often require high doses and frequent administration, leading to adverse side effects [3]. Therefore, there is a pressing need to develop innovative drugs for the treatment of RA.

In RA, various inflammatory cells infiltrate synovial tissues, predominantly macrophages (Mφ), which play a crucial role in pathophysiological responses [4]. The activated pro-inflammatory Mφ subset known as M1Mφ produces a series of inflammatory cytokines, including tumor necrosis factor-α (TNF-α), interleukin-1β (IL-1β), and interleukin-6 (IL-6) [5]. Therefore, M1Mφ is a promising therapeutic target in the symptomatic treatment of RA [6]. Folate-modified silver nanoparticles actively target M1Mφ, mediate a synergistic reduction in M1Mφ and polarization of M2Mφ, and thereby providing an effective treatment alternative [7]. Likewise, punicalagin is also capable of alleviating pathologic inflammation by inhibiting both polarization and pyroptosis phenotypes of M1Mφ via the nuclear factor-kappaB (NF-κB) pathway [8]. The polarization of Mφ involves various molecular mechanisms, one of which is the toll-like receptor 4 (TLR4)/NF-κB pathway [9,10].

Journal of
BIOLOGICAL REGULATORS
and Homeostatic Agents

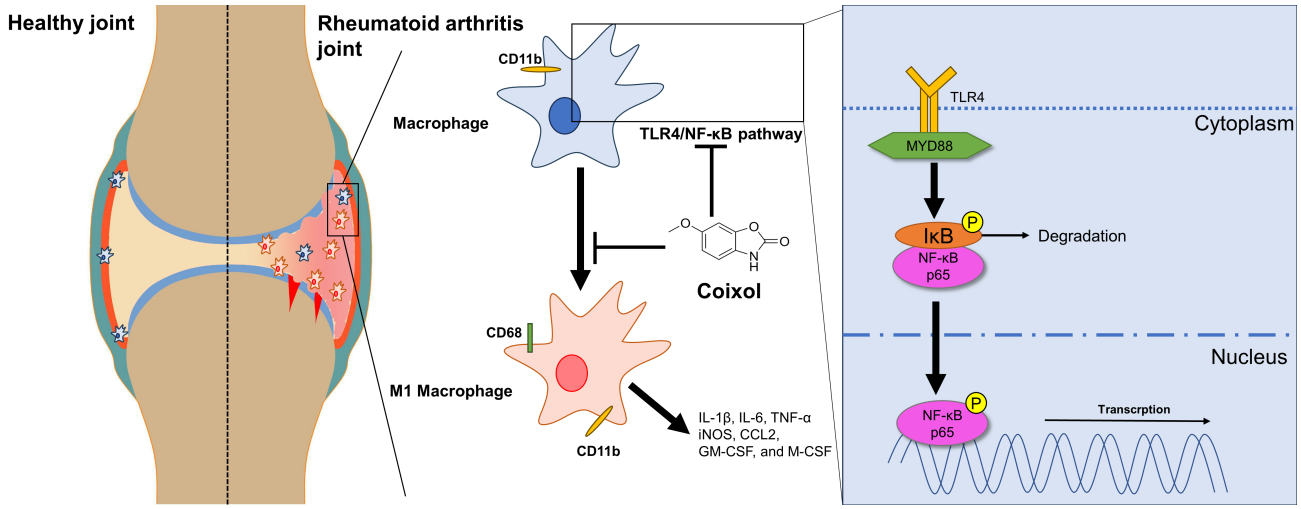

Graphical Abstract.

Berberine has been found to interact with TLR4 to interfere with the TLR4/NFκB signaling pathway, which may be the mechanism by which berberine attenuates inflammation in the early stages [11]. Studies indicated that zanubrutinib inhibits the activation of TLR4/NF-κB signaling pathway, thereby suppressing M1Mφ polarization [12–14]. Similarly, Wilforlide A exhibits anti-inflammatory potential on RA through inhibiting TLR4/NF-κB-mediated M1Mφ polarization [15].

C. lacryma-jobi var. ma-yuen (Rom.Caill.) Stapf is a herbal medicine traditionally used in China. One of its main active ingredients is coixol (COI). Studies have shown that the extract of *C. lacryma-jobi var. ma-yuen* (Rom.Caill.) Stapf has anti-RA effects by inhibiting inflammatory response and alleviating oxidative stress [16,17]. COI has also been found to ameliorate lung injury caused by bacterial infection by interfering with the heat shock protein 70-mediated TLR4/NF-κB signal transduction [18]. Additionally, COI has been demonstrated to inhibit the production of pro-inflammatory factors in lipopolysaccharide (LPS)-induced marophages [19]. Based on these findings, the hypothesis is that COI exerts its therapeutic effect on RA by regulating Mφ polarization. To test this hypothesis, a collagen-induced arthritis (CIA) model in rats was established. The therapeutic effect and the impacts on Mφ polarization in blood, spleen, and synovial joints of COI on CIA rats were examined. The role of COI in regulating M1 polarization in rat bone-marrow-derived Mφ (BMDM) and its regulatory role in the TLR4/NF-κB pathway *in vitro* were also confirmed.

Methods

Basic Information of Animals and Materials Used in This Study

Male Wistar rats (specific pathogen-free grade), aged 6–8 weeks and weighing 200–220 g, were obtained from HuaFukang Biotechnology Co., Ltd. (Permit No. SCXK (Beijing) 2020-0004, Beijing, China). The rats were fed at 22 $\pm$ 2 °C with free access to food and water. Detailed information regarding the reagents and assay kits used in this experiment was as follows.

COI (S31772), Methotrexate (MTX, S18026), and lipopolysaccharide (LPS, S11060) were purchased from YuanYe Biotechnology (Shanghai, China). Resatorvid (TAK242, 614316), Freund's complete adjuvant (F5881) and bovine Type II collagen (CII, 234184-M) were bought from Sigma (Shanghai, China). Interferon-γ (IFN-γ, 400-20) and rat macrophage colony-stimulating factor (M-CSF, 400-28) were purchased from PeproTech China (Suzhou, China). Dulbecco's Modified Eagle's Medium (DMEM, 12100046, Life Technologies, Carlsbad, CA, USA). Fetal bovine serum (FBS, 1943609-65-1, Sigma-Aldrich Co., St. Louis, MO, USA). Red blood cell (RBC) lysis buffer (ab204733, Abcam, Cambridge, UK). Enzyme-linked immunosorbent assay (ELISA) kits of rat TNF-α (ml002859), interleukin-1β (IL-1β, ml028514), IL-6 (ml064292), inducible nitric oxide synthase (iNOS, ml059045), granulocyte macrophage colony-stimulating factor (GM-CSF, ml302827) and M-CSF (ml002980) were bought from Enzyme-linked Biotechnology (Shanghai, China). ELISA kit for chemokine (C-C motif) ligand 2 (CCL2, ab219045) was purchased from Abcam (Cambridge, UK). Flow cytometry antibody for CD11b (17-0112-82) and CD68 (MA5-28262) were purchased from ThermoFisher Scientific (CHINA) (Shanghai, China). Primary antibodies for TLR4 (ab217274), myeloid differentiation primary response 88 (MyD88, ab219413), IkappaB (IκB, ab32518), phosphorylated-IkappaB (p-IκB, ab133462), CD11b (ab238658), and beta-actin (β-actin, ab8226), and relative secondary antibodies including goat anti-rabbit IgG H&L (ab205718), goat anti-rabbit IgG H&L conjugated APC (ab130805) and goat anti-mouse IgG H&L (FITC, ab6785) were obtained from Abcam (Cambridge,

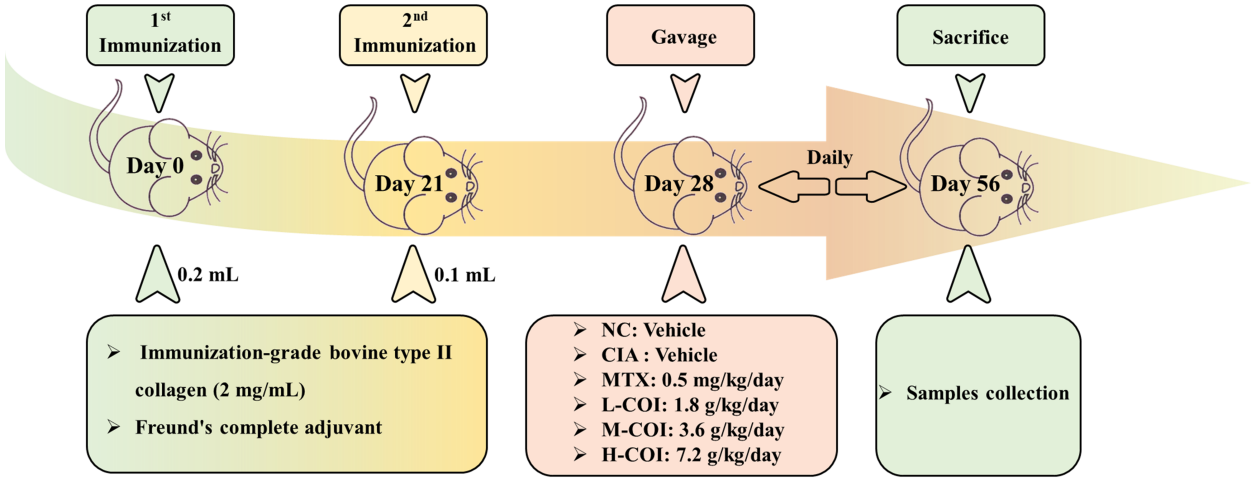

Fig. 1. Experimental design of the *in vivo* study.

Table 1. Evaluation of histopathologic changes.

Feature score	Score	Description
Soft tissue around the joint	0	No abnormality
	1	Mild inflammatory changes
	2	Noticeable inflammatory changes
	3	Significant inflammatory changes
Synovial tissue	0	No abnormality
	1	Mild inflammatory changes
	2	Noticeable inflammatory changes
	3	Significant inflammatory changes
Cartilage	0	No abnormality
	1	Slightly damaged articular cartilage and an intraarticular pannus
	2	Destroyed articular cartilage, lacking local articular cartilage, hyperplastic fibrous tissue and infiltrated neutrophil and lymphocyte
	3	Inflammation accumulated throughout the articular cavity, significantly damaged articular cartilage, seriously hyperplastic fibrous tissue, and locally infiltrated with a large number of neutrophils and lymphocytes

UK). Primary antibody for CD68 (28058-1-AP), p65 (80979-1-RR) and p-p65 (82335-1-RR) were purchased from Proteintech Group (Wuhan, China). Roswell Park Memorial Institute (RPMI) medium (SH30809.01), and Lipofectamine 2000 Reagent (11668030) were obtained from ThermoFisher Scientific (CHINA) (Shanghai, China). 4% formaldehyde solution (P885233, Macklin, Shanghai, China). Electochemiluminescence (ECL) chemiluminescence buffer (PE0010, Solarbio, Beijing, China). Plasmids for NF-κB luciferase reporter (11501ES03), pGMLR-CMV luciferase reporter (11558ES03) and Dual-Luciferase Reporter Gene Assay Kit (11402ES60) were purchased from Yeasen Biotechnology (Shanghai, China).

Animal Experiments

Sixty rats were used in this study. After a 7-day adaptation period, 10 rats were randomly assigned to the normal control (NC) group using the random number table method, while the remaining 50 were used to establish CIA rat model. Freund's complete adjuvant and CII were mixed with equal volume to prepare a collagen emulsion. The emulsion contains 1 mg/mL of CII. On day 0, rats were subcutaneously injected with 0.2 mL of the collagen emulsion at the base of their tails, followed by a booster injection of 0.1 mL on day 21 [20]. The NC group injected with an equal volume of vehicle. An arthritis index score was assessed every 3 days following the first immunization [21], with a score of 6 points indicating successful RA induction. The CIA model was established 28 days after the first injection.

After modeling, CIA model rats were divided into five groups randomly: CIA, MTX, low-dose COI (L-COI), medium-dose COI (M-COI), and high-dose COI (H-COI) using the random number table method. The doses of COI for each group were determined as 1.80, 3.60, and 7.20 g/kg/day, respectively, based on a dose of 42 g/day for human adults weighing 70 kg. The dose for the MTX group

Journal of
BIOLOGICAL REGULATORS
and Homeostatic Agents

was calculated in the same way as MTX 0.5 mg/kg/day. The NC and the CIA groups received a carrier solution of the same volume. Treatments were administered daily from day 28–56 for a total of 28 days. On day 56, rats were anesthetized using 50 mg/kg pentobarbital sodium, and their arthritis index scores and paw volumes were determined. Blood samples, spleens, and bilateral hind ankle joints were obtained from the rats sacrificed by cervical dislocation (Fig. 1). Besides, blood samples were processed by centrifugation at 400 ×g for 15 min to separate the serum. All animal experiments were approved by the Animal Ethics Committee of Jiaxing Hospital of TCM (SL-2021-0012) and conducted following the regulations for the use of experimental animals.

Cell Experiments

Bone marrow-derived macrophages (BMDMs) were isolated and induced from the femur and tibia of rats (12 weeks, 300–350 g) following a previously established protocol [22,23]. Briefly, the leg of the rat was immersed in 75% ethanol, and the femur and tibia were exposed. Then, both ends of the femur and tibia were cut open, and the bone marrow was flushed out using DMEM supplemented with 10% heat-inactivated FBS. The resulting cell suspension was thoroughly mixed with culture media and filtered using a 40 μm nylon mesh filter to collect the cells. This cell suspension was then centrifuged at 400 ×g for 5 min, and the cell precipitate was harvested. Then, RBC lysis buffer was added to cells to remove red blood cells. The cell pellet was resuspended in complete medium containing 0.10 μg/mL of M-CSF and cultured for 7 days to obtain BMDM. The mycoplasma in primary cultured BMDMs was detected using the DNA fluorochrome staining method [(4′,6-diamidino-2-phenylindole (DAPI)-test)] as described previously [24]. The fluorescence could not be detected outside of the nucleus, indicating that cells were not contaminated with mycoplasma.

In order to test the effect of drugs on BMDM polarization, cells were gently removed after induction and seeded into a 24-well plate. The density of cells in 24-well plate was 2×10^5 cells/well. The cells were then incubated in a medium without M-CSF for 24 h before being washed and co-cultured with 100 ng/mL of LPS and 20 ng/mL of interferon (IFN)-γ to induce M1Mφ and the corresponding drugs for 24 h. After culturing, cells and supernatants were collected separately.

ELISA Assay

The levels of IL-1β, TNF-α, IL-6, iNOS, GM-CSF, CCL2, and M-CSF were estimated in the serum or supernatant using a one-step double-antibody sandwich ELISA assay. The specific procedures outlined in the instructions of the reagent kit were followed, and a multimode microplate reader (Varioskan Flash, ThermoScientific, Waltham, MA, USA) was used for the assay.

Pathological Staining and Immunofluorescence (IF) Staining

The ankle was fixed with 4% polyformaldehyde for 48 hours and then immersed in 10% EDTA buffer at 25 °C for 25 days. Then, the ankle samples were embedded in paraffin and sliced longitudinally into 3 μm sections. Routine hematoxylin-eosin (HE) staining was performed. Microscopic images of the sections were observed and captured using a light microscope (ECLIPSE E100, Nikon, Tokyo Metropolis, Japan) for histological analysis. Histopathologic changes were evaluated according to an established method [25], as shown in Table 1. For immunofluorescence (IF) staining, the sections were prepared using the same procedure as that for pathological staining. After deparaffinization, the sections were hydrated with decreasing concentrations of ethanol. Following antigen retrieval, the sections were incubated at 25 °C in a 3% H_2O_2 solution to block the activity of endogenous peroxidase. The sections were incubated in 20% normal goat serum for 1 hour, followed by incubation with primary antibodies including mouse anti-CD11b (1:100) and rabbit anti-CD68 (1:200) at 4 °C for 12 hours. Then, the sections were incubated with relative-fluorescently labeled secondary antibodies at room temperature for 1 hour. Subsequently, the nuclei were stained with DAPI. Regions with positive expression were observed using a fluorescence microscope (BX43, OLYMPUS, Tokyo Metropolis, Japan) and quantified by Image-Pro Plus (version 6.0, Media Cybernetics, Silver Springs, FL, USA).

3-[4,5-Dimethylthiazol-2-yl]-2,5 Diphenyl Tetrazolium Bromide (MTT) Assay

The effect of COI on cell viability was assessed using the MTT assay. Briefly, BMDMs were seeded in a 96-well plate. Then, the cells were incubated with different concentrations of COI (0, 10, 50, 100, 200, 400 μM) for 24 hours. After incubation, 10 μL of MTT solution (5 mg/mL) was added to each well, then an additional 4-hour incubation of the cells was performed. The medium was gently aspirated, and 100 μL of DMSO was added. The absorbances of the samples were then detected at 570 nm using a multimode microplate reader (Varioskan Flash, ThermoScientific, Waltham, MA, USA). The formula of cell viability was as follows:

$$\%\ \text{cell viability} = \frac{A_{COI} - A_{Blank}}{A_{Control} - A_{Blank}} \times 100$$

In the formula, A_{COI}, A_{Blank} and $A_{Control}$ referred to the mean absorbance value of COI intervention, blank, and control, respectively.

Flow Cytometry (FCM)

The spleen of rats was processed to a single-cell suspension by placing it in RPMI medium. The cells were fil-

tered using a 70 μm-cell strainer and washed with RPMI medium. The obtained cell suspension was then centrifuged (400 ×g, 5 min). To lyse red blood cells, the supernatant was removed, and we then treated the cells with RBC lysis buffer. The pellets were resuspended in RPMI medium containing 10% FBS and subsequently counted.

The M1Mφ subtypes were distinguished by detecting the co-expression of surface markers CD68 and CD11b using FCM. Briefly, cells were incubated with FITC-conjugated anti-CD68 (1 μg/10^6 cells) and PE-conjugated anti-CD11b (1 μg/10^6 cells) at 4 °C. After 0.5 hours of incubation, we washed the cells 3 times with the staining buffer. A flow cytometer (FACS Aria-II, BD, Franklin Lakes, NJ, USA) was used for data analysis. The non-specific staining was excluded using antibodies of irrelevant immunoglobulin isotypes as negative controls. At least 1 × 10^4 events were acquired and analyzed using the Treestar FlowJo software (version 10.8.1, Stanford University, Stanford, CA, USA).

Western Blotting

The collected cells were placed in an ice-cold RIPA buffer, and we then homogenized them by sonication to extract total protein. Bicinchoninic acid assay (BCA) kit was used to detect the supernatant protein concentration. After adding protein loading buffer, the proteins were held at 97 °C for 10 min to allow complete denaturation. The denatured proteins were separated using SDS-PAGE and transferred to a PVDF membrane. The membrane was blocked with a solution of 5% non-fat milk for 1 hour and then incubated with the primary antibodies, including TLR4 (1:1000), IκB (1:10,000), MyD88 (1:1000), p-IκB (1:10,000), p65 (1:10,000) and p-p65 (1:10,000), and ACTB (1:1000) overnight at 4 °C refrigerator. It was incubated with the HRP-labeled secondary antibody for another 1 hour at room temperature after washing the incubated membrane 3 times with TBST. After another washing step, the bands were visualized using ECL chemiluminescence and gel imaging system (ChemiDocXRS+, Bio-Rad, Hercules, CA, USA). The protein expression was quantified using Image J (version 1.52a, NIH, Bethesda, MD, USA).

Reverse Transcription-Quantitative Polymerase Chain Reaction (RT-qPCR)

Total RNA was extracted from the cells using a total RNA extraction kit, and then its concentration was determined to characterize the mRNA expression of the target gene. Then, cDNA was obtained using a reverse transcription kit and quantitative polymerase chain reaction (qPCR) was performed. The relative expression of each target gene to *Actb* (actin, beta) was calculated according to the $2^{-\Delta\Delta Ct}$ method. Table 2 lists the required primer sequences.

Table 2. Primer sequences.

Gene		Sequence (5′-3′)
Actb	Forward	AGATGACCCAGATCATGTTTGAGA
	Reverse	GCATGAGGGAGCGCGTAA
Il1b	Forward	ATGCCACCTTTTGACAGTGATG
	Reverse	TGTGCTGCTGCGAGATTTGA
Il6	Forward	AGCCAGAGTCCTTCAGAGAGA
	Reverse	GCCACTCCTTCTGTGACTCC
Tnf	Forward	GATCGGTCCCCAAAGGGATG
	Reverse	CCACTTGGTGGTTTGTGAGTG
Nos2	Forward	TCCTGGACATTACGACCCCT
	Reverse	AGGCCTCCAATCTCTGCCTA
Ccl2	Forward	GCCTGCTGTTCACAGTTGC
	Reverse	GAGTGGGGCGTTAACTGCAT
Csf2	Forward	CTCACCCATCACTGTCACCC
	Reverse	TGAAATTGCCCCGTAGACCC
Csf1	Forward	GCCCTTCTTCGACATGGCT
	Reverse	GTTCTGACACCTCCTTGGCA

Actb, actin, beta; *Il1b*, interleukin 1 beta; *Il6*, interleukin 6; *Tnf*, tumor necrosis factor; *Nos2*, nitric oxide synthase 2; *Ccl2*, C-C motif chemokine ligand 2; *Csf2*, colony stimulating factor 2; *Csf1*, colony stimulating factor 1.

Detection of the Nucleus Transition of NF-κB p65 in Rat BMDMs Using Immunofluorescence

BMDMs were seeded into a 12-well plate. Then, cells were fixed with 4% paraformaldehyde diluted with PBS. Then, the cells were permeated with 1% Triton 100 for 0.5 hours, followed by the addition of 2% BSA for 1 hour. The NF-κB p65 antibody (1:400) was incubated overnight. Then, cells were incubated with secondary antibody at 25 °C for 1.5 hours away from light, washing 3 more times, DAPI was added and incubated at 25 °C for 5 min away from light. After DAPI was removed, PBST was used to wash 4 times. Finally, the cells were observed under a fluorescence microscope (BX43, OLYMPUS, Tokyo Metropolis, Japan), and the nucleus transition of NF-κB p65 was quantified based on Manders' Coefficients using Image-Pro Plus (version 6.0, Media Cybernetics, Silver Springs, FL, USA).

NF-κB Transactivation Assay

The transcriptional activity of NF-κB in BMDMs following COI treatment was measured using the luciferase reporter gene technique. BMDMs were seeded into a 12-well plate. Once the cells became adherent, the culture medium was discarded and replaced with culture medium containing the Lipofectamine 2000 transfection reagent and either a NF-κB luciferase reporter plasmid or a pGMLR-CMV luciferase reporter plasmid. The cells were incubated for 6 h. Subsequently, exposure to LPS + IFN-γ and COI or TAK242 was performed separately for 24 h, and the cells were collected. Lysis buffer was added to lyse

Journal of
BIOLOGICAL REGULATORS
and Homeostatic Agents

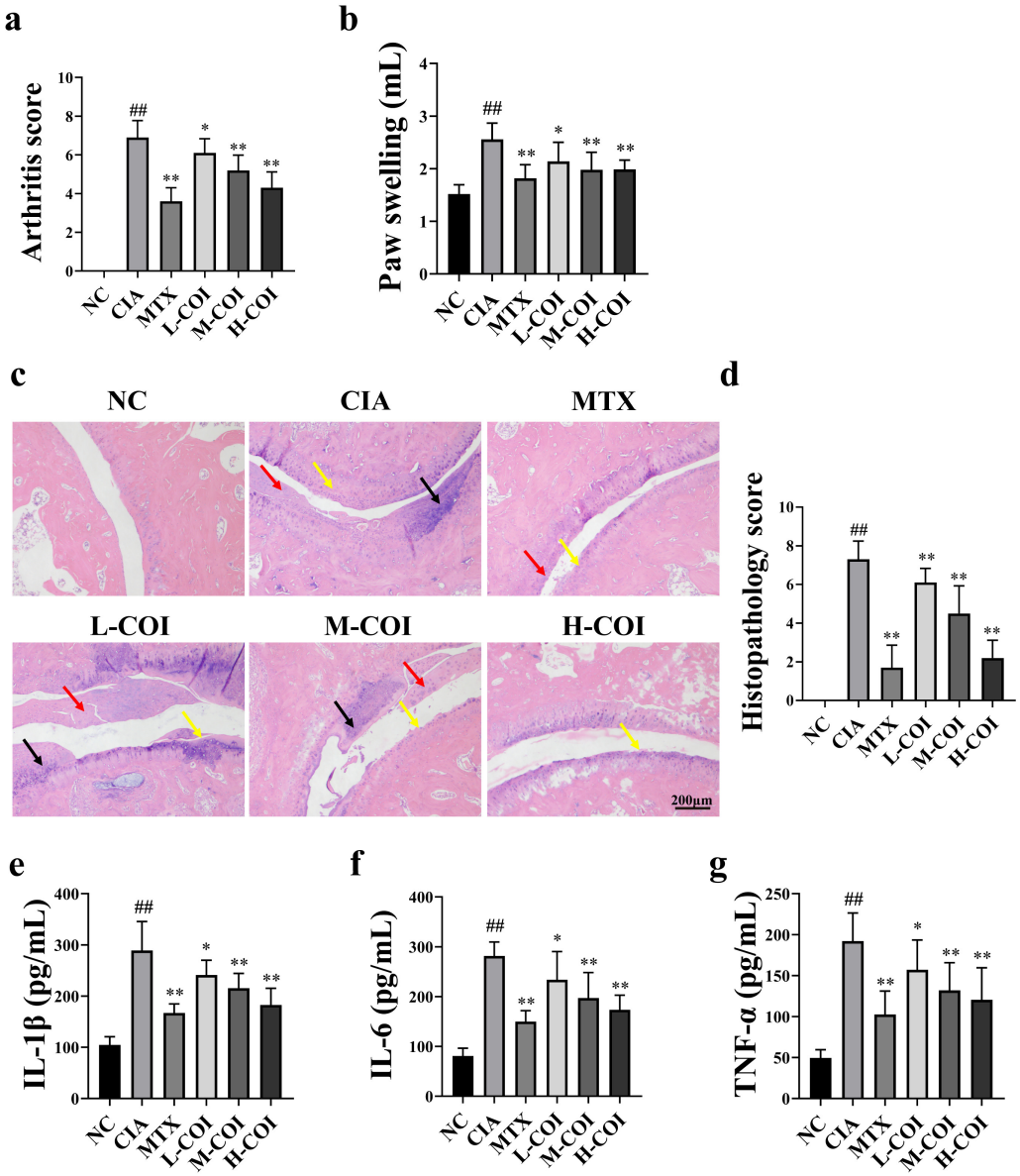

Fig. 2. Coixol (COI) treatment improved rheumatoid arthritis in CIA rats. (a,b) Arthritis score and paw volume. (c) HE staining showed that COI reduced pathological changes in the ankle joint (total magnification: 40×), black arrows indicated inflammatory cell infiltration, red arrows indicated abnormal synovial fibroblast proliferation, and yellow arrows indicated synovial tissue injury. (d) Histopathology scores were assigned to the ankle joints. (e–g) COI treatment resulted in declined levels of IL-1β, IL-6 and TNF-α. ##, $p < 0.01$, compared to NC group; *, $p < 0.05$ and **, $p < 0.01$, compared to CIA group. NC, normal control; CIA, collagen-induced arthritis; MTX, Methotrexate; L-COI, low-dose coixol; M-COI, middle-dose coixol; H-COI, high-dose coixol; IL-1β, interleukin-1β; IL-6, interleukin-6; TNF-α, tumor necrosis factor-α, HE, hematoxylin-eosin.

the cells, and a Dual-Luciferase Reporter Gene Assay Kit was used to measure the luciferase fluorescence intensity of firefly and renilla using a multimode microplate reader (Varioskan Flash, ThermoScientific, Waltham, MA, USA). NF-κB transcriptional activity was the ratio of luciferase fluorescence intensity of firefly to that of renilla. Luciferase activity was normalized to the activity of the internal control.

Data Analysis

SPSS (version 22.0, IBM, Armonk, NY, USA) was used for statistical analysis. All data were shown as mean ± standard deviation (SD). Statistical differences were analyzed using the one-way analysis of variance followed by Tukey's HSD test. Statistically significant was considered with a p value less than 0.05.

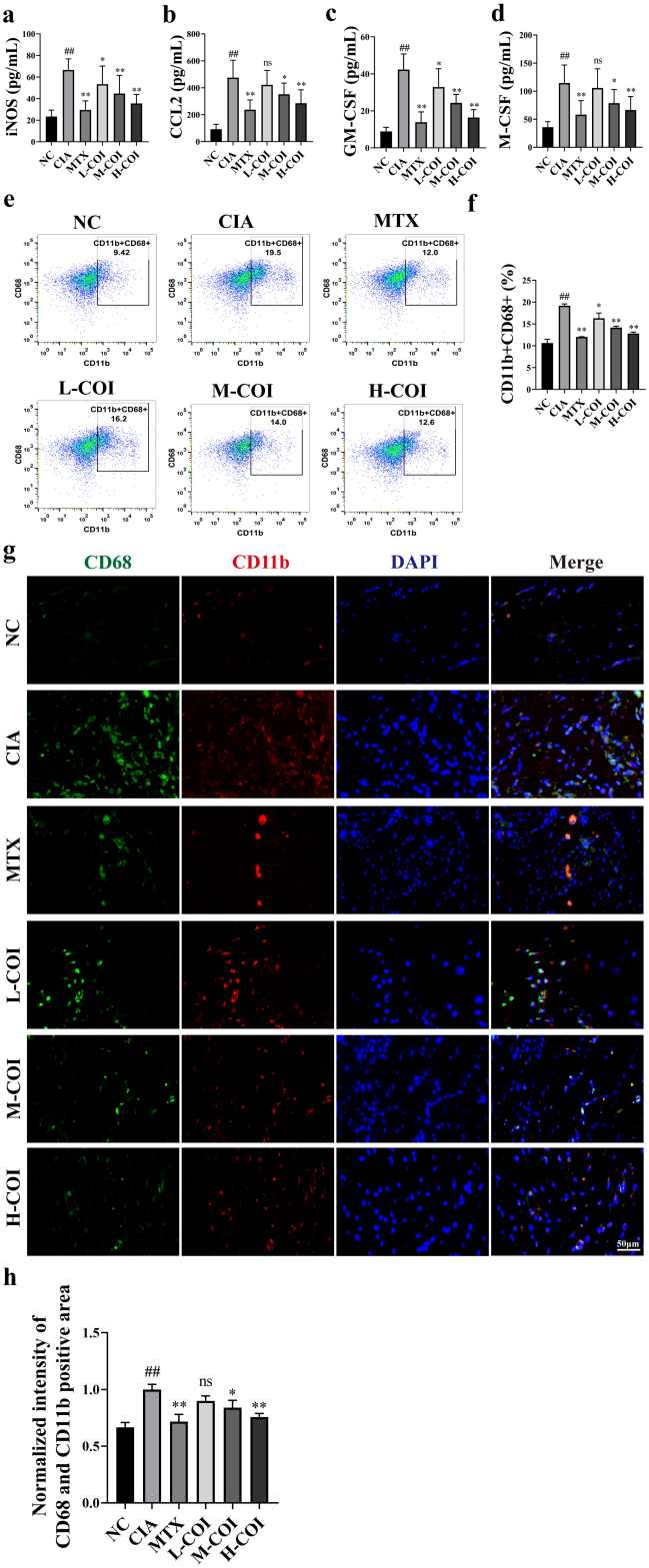

Fig. 3. Coixol treatment altered the polarization of macrophages (Mφ) in the spleen and synovium of CIA rats. (a–d) COI reduced the levels of M1Mφ-related factors iNOS, (C-C motif) ligand 2 (CCL2), GM-CSF, and M-CSF in the serum of CIA rats. (e,f) FCM results indicated that COI reduced the proportion of M1Mφ to Mφ in the spleen. (g,h) Immunofluorescence results indicated that COI reduced the proportion of M1Mφ to Mφ in the synovium (total magnification: 200×). ##, $p < 0.01$, compared to NC group; *, $p < 0.05$, **, $p < 0.01$, and ns, $p > 0.05$, compared to CIA group. iNOS, inducible nitric oxide synthase; CCL2, chemokine (C-C motif) ligand 2; GM-CSF, granulocyte macrophage colony-stimulating factor; M-CSF, macrophage colony-stimulating factor; FCM, flow cytometry; DAPI, 4′,6-diamidino-2-phenylindole.

Journal of
BIOLOGICAL REGULATORS
and Homeostatic Agents

Results

Therapeutic Effects of Coixol on Collagen-Induced Arthritis Rats

After 28 days of treatment, the arthritis index and paw volume of the rats in the CIA group were higher than those of the rats in the NC group ($p < 0.01$, respectively) (Fig. 2a,b). However, both MTX ($p < 0.01$) and COI ($p < 0.05$ in the low-dose coixol (L-COI) group, and $p < 0.01$ in middle-dose coixol (M-COI), high-dose coixol (H-COI) groups) treatments significantly improved the arthritis index and paw swelling. HE staining revealed degeneration and necrosis in synovial cells, abnormal synovial fibroblast proliferation, as well as inflammatory cell infiltration in the synovial tissue. The joint cavity was narrowed with aggregates inside, and the histopathology scores of ankle joints were increased ($p < 0.01$). These symptoms were significantly attenuated in the COI and MTX treatment groups, and the histopathology scores were decreased to varying degrees after COI and MTX treatment ($p < 0.01$, respectively) (Fig. 2c,d). Furthermore, the levels of TNF-α, IL-6, and IL-1β in serum were higher in the CIA than in the other groups ($p < 0.01$, respectively) (Fig. 2e–g). Nevertheless, both MTX and COI treatments could decrease the levels of serum inflammatory factors to varying degrees ($p < 0.05$ in the L-COI group, and $p < 0.01$ in MTX, M-COI, H-COI groups). In the COI treatment group, H-COI showed the most significant therapeutic effect, which was not significantly different from that of the MTX ($p > 0.05$).

Effects of Coixol on the Polarization of Spleen and Synovial Mφ Cells in Collagen-Induced Arthritis Rats

The CIA group has significantly increased serum levels of pro-inflammatory factors iNOS, CCL2, GM-CSF, and M-CSF compared to the NC group ($p < 0.01$, respectively). However, both H-COI and MTX treatment significantly lowered these levels ($p < 0.01$, respectively). Additionally, COI also showed a dose-dependent therapeutic effect (Fig. 3a–d). FCM analysis of spleen cells revealed a significant increase in the ratio of $CD11b^+CD68^+$ in the spleen of CIA rats compared to that in the NC group, indicating an increase in M1Mφ levels in the spleen ($p < 0.01$, respectively). In contrast, both H-COI and MTX significantly reduced the ratio of $CD11b^+CD68^+$ cells in the spleen ($p < 0.01$, respectively) (Fig. 3e,f). Immunofluorescence (IF) results showed that the expression of $CD11b^+CD68^+$ positive cells in the synovial tissue of the CIA group increased compared to that in the NC group ($p < 0.01$, respectively). However, both H-COI and MTX significantly reduced the expression of $CD11b^+CD68^+$ positive cells in the synovial tissue ($p < 0.01$, respectively) (Fig. 3g,h).

Effects of Coixol on the Polarization of BMDM in Rats

The MTT results showed that 10, 50, and 100 μM of COI treatment did not affect the cell viability of rat BMDMs ($p > 0.05$, respectively) (Fig. 4a). Therefore, COI concentrations of 10, 50, and 100 μM were chosen to study BMDM polarization.

To induce M1Mφ polarization in BMDMs, LPS was combined with IFN-γ, and COI was added at different concentrations. FCM results suggested an increase in the ratio of $CD11b^+CD68^+$ cells in BMDMs upon treatment of LPS combined with IFN-γ ($p < 0.01$), indicating successful induction of M1Mφ. Meanwhile, 10 μM, 50 μM and 100 μM of COI treatment decreased the ratio of $CD11b^+CD68^+$ cells ($p < 0.05$, $p < 0.01$, and $p < 0.01$, respectively) (Fig. 4b,c). Furthermore, the levels of inflammatory factors including IL-1β, TNF-α, IL-6, iNOS, CCL2, GM-CSF, and M-CSF in the supernatant of induced BMDMs increased compared to those in untreated cells ($p < 0.01$, respectively) (Fig. 4d–j). COI treatment resulted in a reduction in the levels of inflammatory factors, suggesting that it inhibits M1Mφ polarization. To confirm this, the TLR4 inhibitor TAK242 was selected as a positive control, and no significant difference was found between TAK242 and COI at the concentration of 100 μM in regulating the polarization of rat BMDMs. Thus, we speculated that COI regulates the polarization of rat BMDMs through the TLR4/NF-κB pathway. To test this hypothesis, we applied COI at the concentration of 100 μM in the following experiments.

Inhibitory Effects of Coixol on the TLR4/NF-κB Signaling Pathway in Rat BMDMs

The levels of TLR4, phosphorylated IκB, p65 and MyD88 in cells from different groups were determined using western blotting to observe the inhibitory potential of COI on TLR4/NF-κB pathway in rat BMDMs (Fig. 5a–e). The results suggest that the relative levels of TLR4, phosphorylated IκB, p65 and MyD88 in rat BMDMs induced by LPS combined with IFN-γ were higher than those in the NC group ($p < 0.05$ for p-p65/p65 and $p < 0.01$ for other proteins expression). Furthermore, mRNA levels of interleukin 1 beta (*Il1b*), interleukin 6 (*Il6*), tumor necrosis factor (*Tnf*), nitric oxide synthase 2 (*Nos2*), C-C motif chemokine ligand 2 (*Ccl2*), colony stimulating factor 2 (*Csf2*), and colony stimulating factor 1 (*Csf1*) in the cells increased to various degrees ($p < 0.01$, respectively), indicating the activation of TLR4/NF-κB pathway in BMDMs (Fig. 5f–l). COI or TAK242 administration remarkably decreased the relative levels of TLR4, phosphorylated IκB, p65 and MyD88 ($p < 0.01$, respectively). Moreover, mRNA levels of the related inflammatory factors significantly decreased as well ($p < 0.01$, respectively). Furthermore, no significant differences were found between COI and TAK242 treatment in above-tested indicators ($p > 0.05$, respectively).

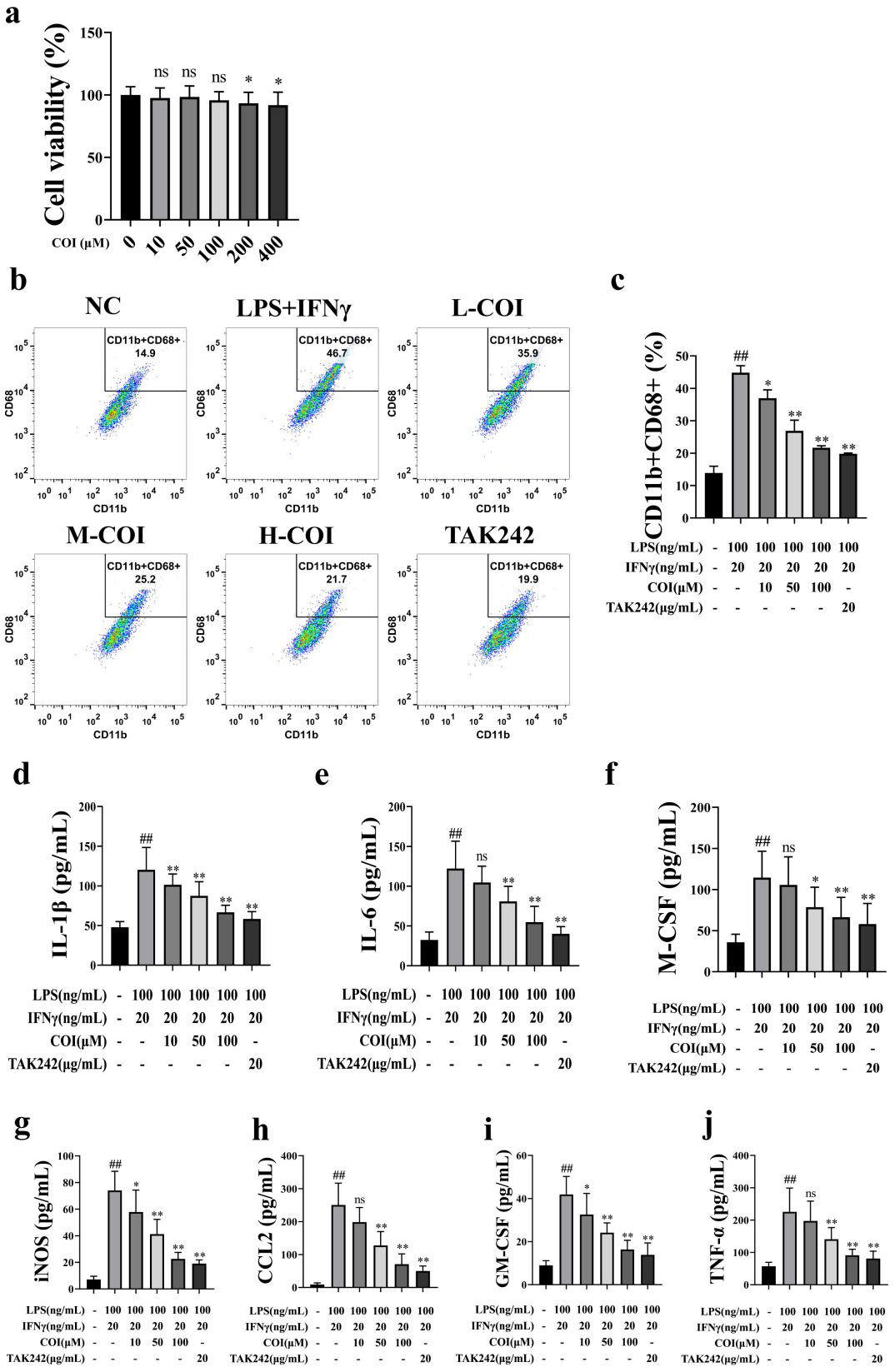

Fig. 4. Coixol treatment altered the polarization of rat bone marrow-derived macrophages (BMDMs). (a) Effect of different doses of COI on cell viability of BMDMs. (b,c) FCM results showed that COI reduced the proportion of M1Mφ to Mφ in LPS + IFN-γ induced BMDMs. (d–j) COI reduced the levels of IL-1β, IL-6, TNF-α, iNOS, CCL2, GM-CSF, and M-CSF in the cell supernatant of BMDMs. ns, $p > 0.05$, compared to COI (0 μM) in Fig. 4a; ##, $p < 0.01$, compared to NC group; *, $p < 0.05$ and **, $p < 0.01$, and ns, $p > 0.05$, compared to LPS + IFN-γ group. LPS, lipopolysaccharide; IFN-γ, interferon-γ; TAK242, resatorvid.

Journal of
BIOLOGICAL REGULATORS
and Homeostatic Agents

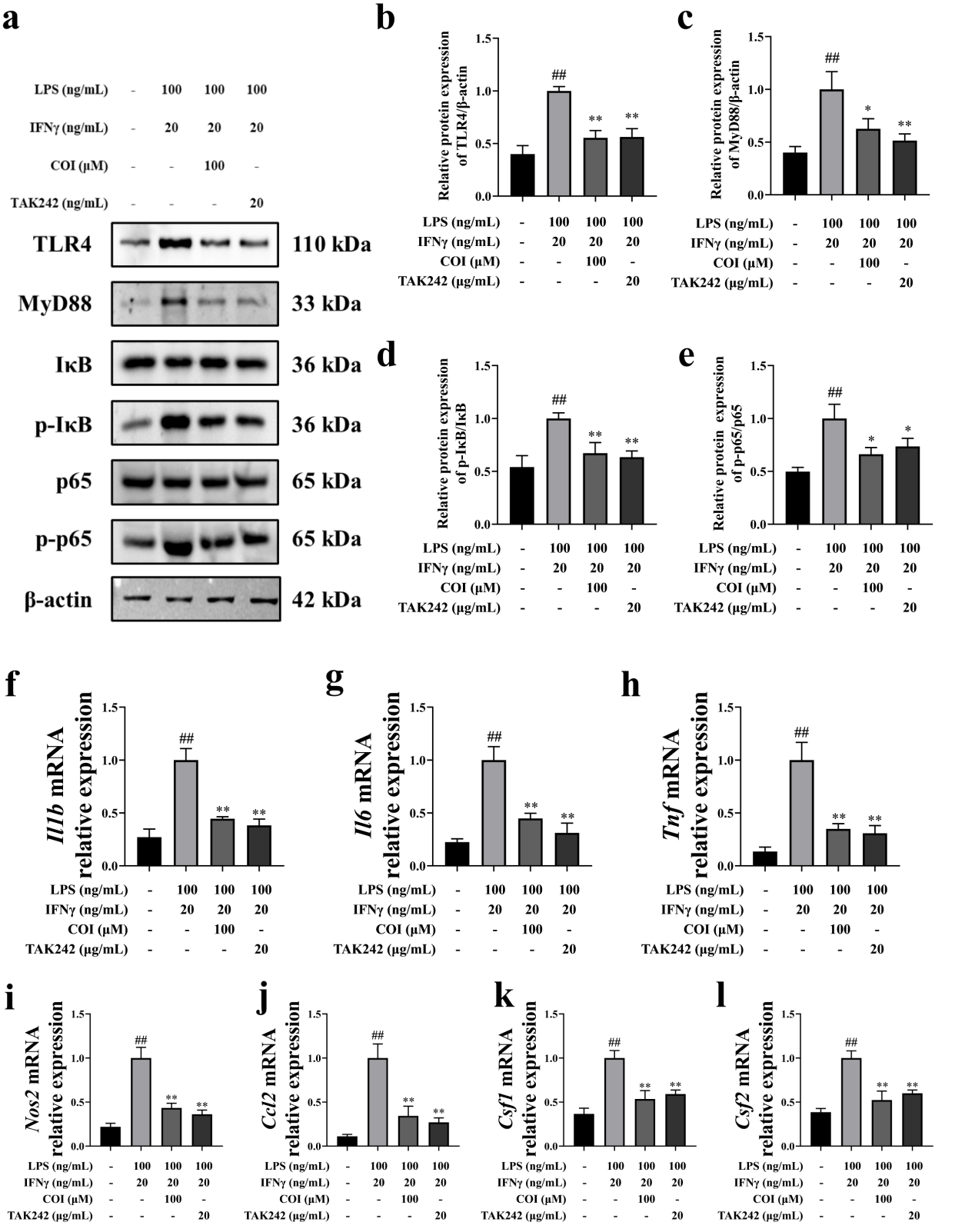

Fig. 5. Coixol treatment improved the toll-like receptor 4 (TLR4)/nuclear factor-kappaB (NF-κB) pathway of rat BMDMs. (a–e) COI reduced the levels of TLR4, MyD88, and phosphorylation of IκB and p65 in LPS + IFN-γ induced rat BMDMs. (f–l) COI reduced the mRNA levels of cytokines *Il1b*, *Il6*, *Tnf*, *Nos2*, *Ccl2*, *Csf2*, and *Csf1* in LPS + IFN-γ induced rat BMDMs. ##, $p < 0.01$, compared to NC group; *, $p < 0.05$, **, $p < 0.01$, compared to LPS + IFN-γ group. MyD88, myeloid differentiation primary response 88; IκB, Ikappa; p-IκB, phosphorylated-IkappaB; β-actin, beta-actin.

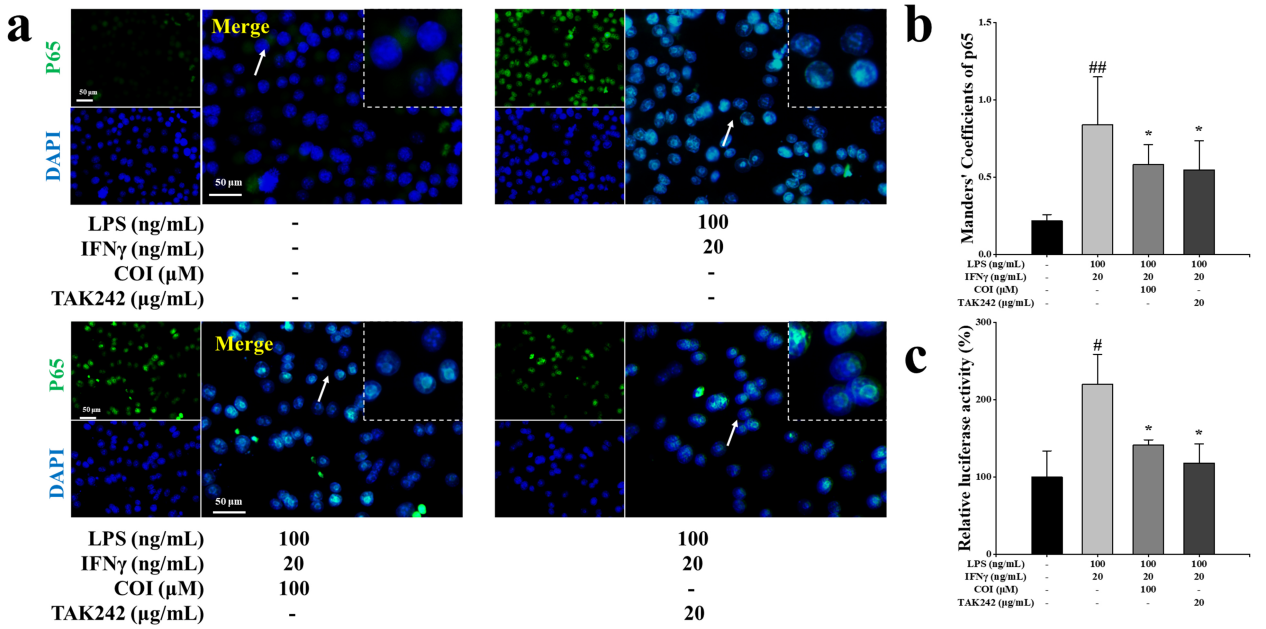

Fig. 6. Coixol inhibited the NF-κB p65 activation of rat BMDMs. (a,b) Immunofluorescence staining showed that COI treatment reduced the nucleus transition of NF-κB p65 in rat BMDMs (total magnification: 200×). White arrows indicate the amplified areas. (c) Luciferase reporter showed that COI treatment reduced the NF-κB transcriptional activity in rat BMDMs. #, $p < 0.05$, and ##, $p < 0.01$, compared to NC group; *, $p < 0.05$, compared to LPS + IFN-γ group.

Effects of Coixol on NF-κB p65 Activation in Rat BMDMs

The effects of COI on NF-κB p65 activation in rat BMDMs were tested using immunofluorescence staining and luciferase reporter assay. The results suggested that LPS combined with IFN-γ increased the positive expression of NF-κB p65 in the nucleus in rat BMDMs compared to untreated cells ($p < 0.01$). However, both COI and TAK242 reduced the positive expression of NF-κB p65 in the nucleus ($p < 0.05$, respectively) (Fig. 6a,b). Furthermore, the luciferase reporter assay suggested that the transcriptional activity of NF-κB in rat BMDMs induced by LPS combined with IFN-γ was also increased compared to that in the NC group ($p < 0.05$), and both COI and TAK242 reduced it ($p < 0.05$) (Fig. 6c).

Discussion

In this study, the therapeutic potential of COI on RA was tested on a CIA rat model. The CIA rat model is widely utilized as a classic and reliable model for studying RA, as it effectively reproduces the autoimmune response to collagen tissue, providing valuable insights into the systemic and chronic progressive nature of RA [26–28]. The CIA rat model closely resembles human RA in terms of clinical symptoms, pathological changes, and immune responses. The model exhibits several pathological features such as symmetric joint involvement, distal limb joint invasion, inflammation due to synovial proliferation, pannus formation, and the destruction of cartilages and bones [29,30]. Inflammatory cytokines have been widely reported to be involved in the development of RA. TNF stimulates the formation of osteoclasts and subsequent degradation of the bone and cartilage [31,32]. TNF strongly induces the release of other pro-inflammatory mediators, including IL-1β, IL-6, and GM-CSF [33]. Blocking TNF results in a rapid decrease in circulating IL-6, which aligns with the hierarchical structure of functional cytokines in the body [34]. IL-6 plays a key role in regulating T-cell migration and activation, as well as downstream inflammatory responses [35]. Studies on the synovial tissue have shown that blocking IL-6 reduces the expression of several chemokines while promoting the expression of repair-promoting factors [36–38]. IL-1 also plays a crucial role in the mechanisms of synovitis and the progressive joint damage leading to RA [39]. Blocking IL-1β has been proposed to facilitate the treatment of certain complications in RA patients [40]. Our research demonstrated that COI treatment significantly improves the arthritis index and reduces paw volume in CIA rats, while significantly lowering the serum levels of inflammatory factors. Additionally, COI ameliorated damage and erosion of the synovial tissue in rats, while reducing the infiltration of inflammatory cells. The conventional drug for RA treatment, MTX, was also tested [41]. MTX has

Journal of
BIOLOGICAL REGULATORS
and Homeostatic Agents

multiple therapeutic roles in RA, such as folic acid antagonism, regulation of inflammatory signal transduction pathways, bone protection, and maintenance of immune system functionality [42]. No significant differences were detected between MTX and H-COI treated rats in terms of improving CIA and reducing inflammation.

The polarization of Mφ plays a vital role in RA [43] and the inflammatory process in the peripheral blood and synovial tissue is mediated and sustained by M1Mφs [44]. M1Mφs are characterized by high expression of CD86, and CD80, and secretion of various kinds of pro-inflammatory mediators [45]. Important markers of M1Mφ activation include iNOS and CCL2, which are significantly elevated in the serum of RA patients [46,47]. Additionally, GM-CSF and M-CSF are cytokines secreted by Mφ [48], and the levels of both GM-CSF and M-CSF are elevated in RA patients [49]. The synovial membrane contains Mφ and infiltrating monocyte-derived Mφ, which play a crucial role in chronic synovitis in RA [50]. These cells regulate immune responses, release pro-inflammatory mediators involved in the inflammatory cascade, activate osteoclasts and fibroblasts, and contribute to joint damage and the chronic nature of the disease [4,51]. The crosstalk between activated M1Mφ and Th1 cells promotes the production of various pro-inflammatory mediators including TNFα, IL-1β, IL-23, IL-6, CXCLs, and CCLs [4]. The spleen also plays a crucial role in regulating systemic inflammation. The spleen receives signals from the parasympathetic nervous system, and the activation of the vagus nerve might inhibit spleen Mφ from producing TNF-α via the celiac-superior mesenteric plexus [52]. Therefore, the depletion of M1Mφ in target organs could serve as a promising biomarker for therapeutic response [53]. Here, we demonstrated that COI treatment significantly improves the levels of pro-inflammatory factors iNOS, CCL2, GM-CSF, and M-CSF in the serum, while reducing the number of M1Mφ in the spleen and synovial tissue in CIA rats. In addition, COI was found to reduce the ratio of BMDM polarizing toward M1Mφ upon induction by LPS and IFN-γ, as well as the levels of multiple released inflammatory factors. These findings indicate that COI can inhibit the M1 polarization of Mφ. Furthermore, the effects of COI at certain concentrations were not significantly different from those of MTX *in vivo* or the TLR4 inhibitor TAK-242 *in vitro*.

TLRs belong to the heterogenous receptor family, and are expressed in cytoplasm or on cell membrane of antigen-presenting cells, including Mφ [54,55]. They play a crucial role in recognizing pathogen-associated molecular patterns to initiate host defense against infections. TLR4 is a key member involved in pathogen recognition [56]. Additionally, TLR4 expression on Mφ facilitates the recognition of RA-associated endogenous antibodies. This triggers intracellular signal transduction involving proteins such as MyD88, IκB, and p65 and thereby leads to NF-κB activation and rapid transcription of pro-inflammatory genes [57,58]. Here, we found that COI reduces the levels of proteins involved in the TLR4/NF-κB pathway in rat BMDMs challenged with LPS and IFN-γ *in vitro*. Additionally, we found that COI reduces the mRNA levels of a series of intracellular inflammatory factors. Furthermore, we found that COI reduced the nucleus transition and transcriptional activity of NF-κB p65. All these findings suggest that the effects of COI may be associated with the regulation of the TLR4/NF-κB signaling pathway.

Conclusions

COI exhibits a significant therapeutic effect on RA. The anti-inflammatory mechanism of COI on RA is associated with inhibiting TLR4/NF-κB-mediated M1Mφ polarization.

Availability of Data and Materials

All the data generated during this study has been presented in this manuscript.

Author Contributions

BXW: investigation, writing-original draft. JLC: investigation, writing-original draft. XJG: investigation, validation, data curation. XLS: investigation, validation, formal analysis. CXN: visualization, data curation. LP: conceptualization, writing-review & editing. FQ: conceptualization, writing-review & editing, funding acquisition. All authors contributed to editorial changes in the manuscript. All authors read and approved the final manuscript. All authors have participated sufficiently in the work to take public responsibility for appropriate portions of the content and agreed to be accountable for all aspects of the work in ensuring that questions related to its accuracy or integrity.

Ethics Approval and Consent to Participate

All animal experiments were approved by the Animal Ethics Committee of Jiaxing Hospital of TCM (SL-2021-0012) and conducted by the regulations for the use of experimental animals.

Acknowledgment

Not applicable.

Funding

This research was funded by the public welfare category projects of Jiaxing Science and Technology Bureau (2022AD10005).

Conflict of Interest

The authors declare no conflict of interest.

References

[1] McInnes IB, Schett G. The pathogenesis of rheumatoid arthritis. The New England Journal of Medicine. 2011; 365: 2205–2219.
[2] Firestein GS. Evolving concepts of rheumatoid arthritis. Nature. 2003; 423: 356–361.
[3] Smolen JS, Steiner G. Therapeutic strategies for rheumatoid arthritis. Nature Reviews. Drug Discovery. 2003; 2: 473–488.
[4] Udalova IA, Mantovani A, Feldmann M. Macrophage heterogeneity in the context of rheumatoid arthritis. Nature Reviews. Rheumatology. 2016; 12: 472–485.
[5] McInnes IB, Schett G. Cytokines in the pathogenesis of rheumatoid arthritis. Nature Reviews. Immunology. 2007; 7: 429–442.
[6] Smolen JS, Aletaha D, Koeller M, Weisman MH, Emery P. New therapies for treatment of rheumatoid arthritis. Lancet. 2007; 370: 1861–1874.
[7] Yang Y, Guo L, Wang Z, Liu P, Liu X, Ding J, *et al*. Targeted silver nanoparticles for rheumatoid arthritis therapy via macrophage apoptosis and Re-polarization. Biomaterials. 2021; 264: 120390.
[8] Ge G, Bai J, Wang Q, Liang X, Tao H, Chen H, *et al*. Punicalagin ameliorates collagen-induced arthritis by downregulating M1 macrophage and pyroptosis via NF-κB signaling pathway. Science China. Life Sciences. 2022; 65: 588–603.
[9] Wang C, Ma C, Gong L, Guo Y, Fu K, Zhang Y, *et al*. Macrophage Polarization and Its Role in Liver Disease. Frontiers in Immunology. 2021; 12: 803037.
[10] Wanderley CW, Colón DF, Luiz JPM, Oliveira FF, Viacava PR, Leite CA, *et al*. Paclitaxel Reduces Tumor Growth by Reprogramming Tumor-Associated Macrophages to an M1 Profile in a TLR4-Dependent Manner. Cancer Research. 2018; 78: 5891–5900.
[11] Gong J, Li J, Dong H, Chen G, Qin X, Hu M, *et al*. Inhibitory effects of berberine on proinflammatory M1 macrophage polarization through interfering with the interaction between TLR4 and MyD88. BMC Complementary and Alternative Medicine. 2019; 19: 314.
[12] Li X, Wei Y, Li S, Liang J, Liu Z, Cui Y, *et al*. Zanubrutinib ameliorates lipopolysaccharide-induced acute lung injury via regulating macrophage polarization. International Immunopharmacology. 2022; 111: 109138.
[13] Li W, Zhu S, Liu J, Liu Z, Zhou H, Zhang Q, *et al*. Zanubrutinib Ameliorates Cardiac Fibrosis and Inflammation Induced by Chronic Sympathetic Activation. Molecules. 2023; 28: 6035.
[14] Zeng KW, Gu MY. Annual advances of integrative pharmacology in 2020. Traditional Medicine Research. 2021; 6: 1–12.
[15] Cao Y, Liu J, Huang C, Tao Y, Wang Y, Chen X, *et al*. Wilforlide A ameliorates the progression of rheumatoid arthritis by inhibiting M1 macrophage polarization. Journal of Pharmacological Sciences. 2022; 148: 116–124.
[16] Zhang C, Zhang W, Shi R, Tang B, Xie S. *Coix lachryma-jobi* extract ameliorates inflammation and oxidative stress in a complete Freund's adjuvant-induced rheumatoid arthritis model. Pharmaceutical Biology. 2019; 57: 792–798.
[17] Yue J, Wang S. Antiinflammatory and analgesic effects and mechanisms of coix seed and its components in adjuvant arthritis rats. Chinese Journal of Tissue Engineering Research. 2023; 27: 4187.
[18] Shen XY, Lu JM, Lu YN, Jin GN, Ma JW, Wang JH, *et al*. Coixol ameliorates Toxoplasma gondii infection-induced lung injury by interfering with T. gondii HSP70/TLR4/NF-κB signaling pathway. International Immunopharmacology. 2023; 118: 110031.
[19] Hu Y, Zhou Q, Liu T, Liu Z. Coixol Suppresses NF-κB, MAPK Pathways and NLRP3 Inflammasome Activation in Lipopolysaccharide-Induced RAW 264.7 Cells. Molecules. 2020; 25: 894.
[20] Ba X, Huang Y, Shen P, Huang Y, Wang H, Han L, *et al*. WTD Attenuating Rheumatoid Arthritis *via* Suppressing Angiogenesis and Modulating the PI3K/AKT/mTOR/HIF-1α Pathway. Frontiers in Pharmacology. 2021; 12: 696802.
[21] Lin TT, Sung YL, Syu JY, Lin KY, Hsu HJ, Liao MT, *et al*. Anti-Inflammatory and Antiarrhythmic Effects of Beta Blocker in a Rat Model of Rheumatoid Arthritis. Journal of the American Heart Association. 2020; 9: e016084.
[22] Barrett JP, Costello DA, O'Sullivan J, Cowley TR, Lynch MA. Bone marrow-derived macrophages from aged rats are more responsive to inflammatory stimuli. Journal of Neuroinflammation. 2015; 12: 67.
[23] Erwig LP, Kluth DC, Walsh GM, Rees AJ. Initial cytokine exposure determines function of macrophages and renders them unresponsive to other cytokines. Journal of Immunology. 1998; 161: 1983–1988.
[24] Uphoff CC, Gignac SM, Drexler HG. Mycoplasma contamination in human leukemia cell lines. I. Comparison of various detection methods. Journal of Immunological Methods. 1992; 149: 43–53.
[25] Jing M, Yang J, Zhang L, Liu J, Xu S, Wang M, *et al*. Celastrol inhibits rheumatoid arthritis through the ROS-NF-κB-NLRP3 inflammasome axis. International Immunopharmacology. 2021; 98: 107879.
[26] Wang Q, Ye C, Sun S, Li R, Shi X, Wang S, *et al*. Curcumin attenuates collagen-induced rat arthritis via anti-inflammatory and apoptotic effects. International Immunopharmacology. 2019; 72: 292–300.
[27] Zhou J, Mao Y, Shi X, Zhang Y, Yu X, Liu X, *et al*. Peimine suppresses collagen-induced arthritis, activated fibroblast-like synoviocytes and TNFα-induced MAPK pathways. International Immunopharmacology. 2022; 111: 109181.
[28] Zhang Q, Peng W, Wei S, Wei D, Li R, Liu J, *et al*. Guizhi-Shaoyao-Zhimu decoction possesses anti-arthritic effects on type II collagen-induced arthritis in rats via suppression of inflammatory reactions, inhibition of invasion & migration and induction of apoptosis in synovial fibroblasts. Biomedicine & Pharmacotherapy. 2019; 118: 109367.
[29] Choudhary N, Bhatt LK, Prabhavalkar KS. Experimental animal models for rheumatoid arthritis. Immunopharmacology and Immunotoxicology. 2018; 40: 193–200.
[30] Holmdahl R, Andersson ME, Goldschmidt TJ, Jansson L, Karlsson M, Malmström V, *et al*. Collagen induced arthritis as an experimental model for rheumatoid arthritis. Immunogenetics, pathogenesis and autoimmunity. Acta Pathologica, Microbiologica, et Immunologica Scandinavica. 1989; 97: 575–584.
[31] Radner H, Aletaha D. Anti-TNF in rheumatoid arthritis: an overview. Wiener Medizinische Wochenschrift. 2015; 165: 3–9.
[32] Rubbert-Roth A, Atzeni F, Masala IF, Caporali R, Montecucco C, Sarzi-Puttini P. TNF inhibitors in rheumatoid arthritis and spondyloarthritis: Are they the same? Autoimmunity Reviews. 2018; 17: 24–28.
[33] Bertolini DR, Nedwin GE, Bringman TS, Smith DD, Mundy GR. Stimulation of bone resorption and inhibition of bone formation in vitro by human tumour necrosis factors. Nature. 1986; 319: 516–518.
[34] Charles P, Elliott MJ, Davis D, Potter A, Kalden JR, Antoni C, *et al*. Regulation of cytokines, cytokine inhibitors, and acute-phase proteins following anti-TNF-alpha therapy in rheumatoid arthritis. Journal of Immunology. 1999; 163: 1521–1528.
[35] Ohshima S, Saeki Y, Mima T, Sasai M, Nishioka K, Nomura S, *et al*. Interleukin 6 plays a key role in the development of antigen-induced arthritis. Proceedings of the National Academy of Sciences of the United States of America. 1998; 95: 8222–8226.
[36] Kondo N, Kuroda T, Kobayashi D. Cytokine Networks in the

Journal of
BIOLOGICAL REGULATORS
and Homeostatic Agents

Pathogenesis of Rheumatoid Arthritis. International Journal of Molecular Sciences. 2021; 22: 10922.

[37] Mateen S, Zafar A, Moin S, Khan AQ, Zubair S. Understanding the role of cytokines in the pathogenesis of rheumatoid arthritis. Clinica Chimica Acta. 2016; 455: 161–171.

[38] Ducreux J, Durez P, Galant C, Nzeusseu Toukap A, Van den Eynde B, Houssiau FA, *et al*. Global molecular effects of tocilizumab therapy in rheumatoid arthritis synovium. Arthritis & Rheumatology. 2014; 66: 15–23.

[39] Gabay C. IL-1 inhibitors: novel agents in the treatment of rheumatoid arthritis. Expert Opinion on Investigational Drugs. 2000; 9: 113–127.

[40] Ruscitti P, Cipriani P, Liakouli V, Carubbi F, Berardicurti O, Di Benedetto P, *et al*. The Emerging Role of IL-1 Inhibition in Patients Affected by Rheumatoid Arthritis and Diabetes. Reviews on Recent Clinical Trials. 2018; 13: 210–214.

[41] Burmester GR, Pope JE. Novel treatment strategies in rheumatoid arthritis. Lancet. 2017; 389: 2338–2348.

[42] Zhao Z, Hua Z, Luo X, Li Y, Yu L, Li M, *et al*. Application and pharmacological mechanism of methotrexate in rheumatoid arthritis. Biomedicine & Pharmacotherapy. 2022; 150: 113074.

[43] Tardito S, Martinelli G, Soldano S, Paolino S, Pacini G, Patane M, *et al*. Macrophage M1/M2 polarization and rheumatoid arthritis: A systematic review. Autoimmunity Reviews. 2019; 18: 102397.

[44] Ross EA, Devitt A, Johnson JR. Macrophages: The Good, the Bad, and the Gluttony. Frontiers in Immunology. 2021; 12: 708186.

[45] Arango Duque G, Descoteaux A. Macrophage cytokines: involvement in immunity and infectious diseases. Frontiers in Immunology. 2014; 5: 491.

[46] Xue Q, Yan Y, Zhang R, Xiong H. Regulation of iNOS on Immune Cells and Its Role in Diseases. International Journal of Molecular Sciences. 2018; 19: 3805.

[47] Park SY, Lee SW, Lee SY, Hong KW, Bae SS, Kim K, *et al*. SIRT1/Adenosine Monophosphate-Activated Protein Kinase α Signaling Enhances Macrophage Polarization to an Anti-inflammatory Phenotype in Rheumatoid Arthritis. Frontiers in Immunology. 2017; 8: 1135.

[48] Gasson JC. Molecular physiology of granulocyte-macrophage colony-stimulating factor. Blood. 1991; 77: 1131–1145.

[49] Ushach I, Zlotnik A. Biological role of granulocyte macrophage colony-stimulating factor (GM-CSF) and macrophage colony-stimulating factor (M-CSF) on cells of the myeloid lineage. Journal of Leukocyte Biology. 2016; 100: 481–489.

[50] Boutet MA, Courties G, Nerviani A, Le Goff B, Apparailly F, Pitzalis C, *et al*. Novel insights into macrophage diversity in rheumatoid arthritis synovium. Autoimmunity Reviews. 2021; 20: 102758.

[51] Herenius MMJ, Thurlings RM, Wijbrandts CA, Bennink RJ, Dohmen SE, Voermans C, *et al*. Monocyte migration to the synovium in rheumatoid arthritis patients treated with adalimumab. Annals of the Rheumatic Diseases. 2011; 70: 1160–1162.

[52] Rosas-Ballina M, Ochani M, Parrish WR, Ochani K, Harris YT, Huston JM, *et al*. Splenic nerve is required for cholinergic anti-inflammatory pathway control of TNF in endotoxemia. Proceedings of the National Academy of Sciences of the United States of America. 2008; 105: 11008–11013.

[53] Kinne RW, Stuhlmüller B, Burmester GR. Cells of the synovium in rheumatoid arthritis. Macrophages. Arthritis Research & Therapy. 2007; 9: 224.

[54] West AP, Brodsky IE, Rahner C, Woo DK, Erdjument-Bromage H, Tempst P, *et al*. TLR signalling augments macrophage bactericidal activity through mitochondrial ROS. Nature. 2011; 472: 476–480.

[55] Krutzik SR, Tan B, Li H, Ochoa MT, Liu PT, Sharfstein SE, *et al*. TLR activation triggers the rapid differentiation of monocytes into macrophages and dendritic cells. Nature Medicine. 2005; 11: 653–660.

[56] Park SY, Lee SW, Baek SH, Lee CW, Lee WS, Rhim BY, *et al*. Suppression of PU.1-linked TLR4 expression by cilostazol with decrease of cytokine production in macrophages from patients with rheumatoid arthritis. British Journal of Pharmacology. 2013; 168: 1401–1411.

[57] Takeda K, Akira S. Toll-like receptors. Current Protocols in Immunology. 2015; 109: 14.12.1–14.12.10.

[58] Zeng MY, Tong QY. Anti-inflammation Effects of Sinomenine on Macrophages through Suppressing Activated TLR4/NF-κB Signaling Pathway. Current Medical Science. 2020; 40: 130–137.